



Cite this: *Chem. Commun.*, 2014, 50, 12768

Received 4th July 2014,  
Accepted 25th August 2014

DOI: 10.1039/c4cc05143b

www.rsc.org/chemcomm

## Distance dependent charge separation and recombination in semiconductor/molecular catalyst systems for water splitting†

Anna Reynal,<sup>\*a</sup> Janina Willkomm,<sup>b</sup> Nicoleta M. Muresan,<sup>b</sup> Fezile Lakadamyali,<sup>b</sup> Miquel Planells,<sup>a</sup> Erwin Reisner<sup>\*b</sup> and James R. Durrant<sup>\*a</sup>

**The photoinduced reduction of three Co electrocatalysts immobilised on TiO<sub>2</sub> is 10<sup>4</sup> times faster than the reverse charge recombination. Both processes show an exponential dependence on the distance between the semiconductor and the catalytic core.**

The immobilisation of molecular catalysts on semiconductors for solar fuel production is an attractive strategy to exploit electrocatalysts in a heterogeneous photocatalytic environment. Efficient H<sub>2</sub> production in such hybrid systems requires effective electronic coupling between the light harvesting unit and the electrocatalyst. Current examples based on non-precious metal complexes include Co, Ni and Fe electrocatalysts attached to narrow band-gap or dye-loaded wide band-gap semiconductors that allow for visible light absorption.<sup>1</sup> In order to reduce protons to H<sub>2</sub> through a mononuclear heterolytic route, the semiconductors have to transfer two electrons to one molecular catalyst. Previously, we reported that recombination of the reduced catalyst with valence band holes in the semiconductor limits the efficiency in these photocatalytic systems.<sup>2</sup> Thus, achieving essentially uni-directional (vectorial) electron transfer from the semiconductor to the catalyst is crucial for enhancing long-lived charge separation and allowing the slow catalytic reactions to take place before electron-hole recombination.

Understanding and controlling the influence of the molecular structure on interfacial electron transfer dynamics has been a key requirement to enhance the efficiency of dye sensitised solar cells (DSSCs).<sup>3</sup> Analogously to DSSCs, one might expect that changes in the molecular structure of the catalyst in such hybrid systems for solar fuels will also affect the kinetics of charge separation and recombination<sup>4</sup> (in reverse direction of charge separation compared to DSSCs, see Fig. 1). However, systematic

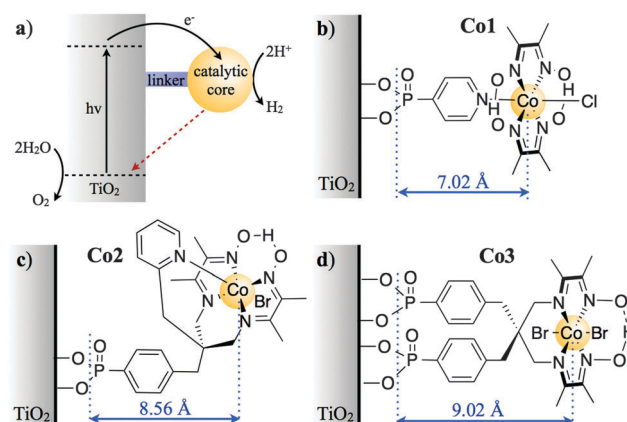


**Fig. 1** (a) Electron transfer processes in TiO<sub>2</sub> functionalised with a molecular catalyst for H<sub>2</sub> production after UV-light excitation. The solid black and dashed red arrows indicate charge separation and recombination, respectively. Molecular structures of the catalysts for H<sup>+</sup> reduction are shown in (b) for **Co1**, (c) for **Co2** and (d) for **Co3** (charges omitted for clarity). The blue arrows indicate the distance between the anchoring groups and the catalyst metal centre (*r*, Å), as determined by energy minimised DFT calculations (Fig. S1, ESI†).‡

studies addressing the effect of molecular structure of the catalyst on charge transfer dynamics are scarce. In this study, we compare the kinetics of charge separation and recombination when a semiconductor (TiO<sub>2</sub>) is functionalised with three related cobalt electrocatalysts, whose molecular structure varies the physical separation between the catalytic core and the semiconductor surface (Fig. 1). In this hybrid system, the semiconductor acts as light harvester and the H<sub>2</sub> evolution is driven by the anchored molecular catalyst.

The molecular catalysts and nanocrystalline anatase TiO<sub>2</sub> films employed herein were synthesised as reported elsewhere.<sup>5</sup> Functionalisation of the TiO<sub>2</sub> films with a monolayer of molecular catalyst (ca. 900 molecules of **Co1**, 1000 of **Co2** and 1050 of **Co3** per TiO<sub>2</sub> particle, see ESI† for detailed calculations) was achieved by dipping the films into 10<sup>-4</sup> M catalyst aqueous solutions for 12 h at rt in the dark. The kinetics of charge separation were studied by monitoring the photogenerated charge carriers (electrons and holes) in the

<sup>a</sup> Department of Chemistry, Imperial College London, Exhibition Road, London SW7 2AZ, UK. E-mail: a.reynal@imperial.ac.uk, j.durrant@imperial.ac.uk

<sup>b</sup> Christian Doppler Laboratory for Sustainable SynGas, Department of Chemistry, University of Cambridge, Cambridge CB2 1EW, UK. E-mail: reisner@ch.cam.ac.uk

† Electronic supplementary information (ESI) available: Experimental details, DFT calculations and additional transient absorption measurements. See DOI: 10.1039/c4cc05143b



nanostructured TiO<sub>2</sub> films by transient absorption (TA) spectroscopy with a set-up described previously.<sup>5d</sup> No signals directly from the Co catalysts were apparent over the spectral range studied. The signal corresponding to holes in TiO<sub>2</sub> has a maximum at 460 nm, and electrons can be monitored at 900 nm.<sup>6</sup>

Electron transfer from the semiconductor to the molecular Co catalyst was first confirmed by TA measurements in the presence of a 0.1 M triethanolamine (TEOA) solution as hole scavenger. A lifetime of photoexcited TiO<sub>2</sub> electrons of ~1 s was observed on bare TiO<sub>2</sub> films due to suppression of electron–hole recombination in the semiconductor. When TiO<sub>2</sub> was functionalised with a Co electrocatalyst, the lifetime of photogenerated electrons in the semiconductor is reduced by ≥3 orders of magnitude, assigned to interfacial electron transfer to the molecular catalyst (Fig. 2). We note significant differences in the kinetics of this electron transfer upon the molecular catalyst employed. Thus,  $t_{50\%}$  is ~5 μs for Co1, 4 times slower for Co2 ( $t_{50\%}$  ~ 20 μs) and 10 times slower for Co3 ( $t_{50\%}$  ~ 50 μs) (Fig. S2, ESI† and further discussed below).

The kinetics of charge recombination of electrons transferred to the catalytic centre with TiO<sub>2</sub> valence band holes is only observed in the absence of chemical scavengers, so that the holes are not removed from the semiconductor. Conditions free of sacrificial agents are particularly relevant to coupling catalytic proton reduction to water oxidation, where the slow timescales of water oxidation will result in significant hole accumulation on the semiconductor. In an aqueous solution without hole scavenger, the decay of photogenerated electrons and holes in bare TiO<sub>2</sub> presents identical kinetics on the micro- to milli-second timescales assigned to bimolecular recombination of these charge carriers through trapping–detrapping processes (Fig. S3, ESI†).<sup>7</sup> Consistent with previous studies, band-gap excitation of the catalyst-loaded TiO<sub>2</sub> showed smaller signal amplitudes and faster decays for photoexcited electrons compared to the bare metal oxides (Fig. 3).<sup>2</sup> This behaviour is assigned to the transfer

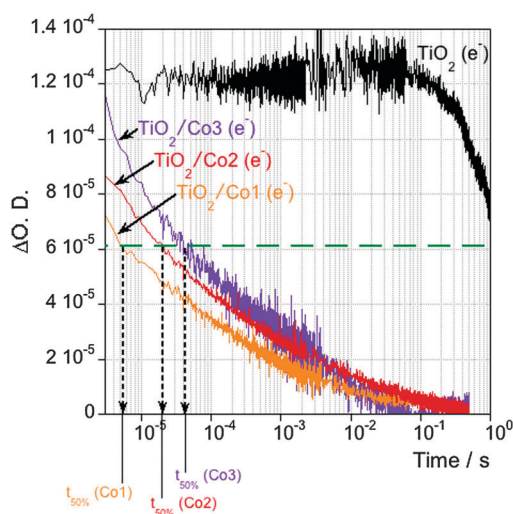


Fig. 2 TA decays corresponding to photoexcited electrons in the TiO<sub>2</sub> for bare films (black trace) and when functionalised with Co1 (orange trace), Co2 (red trace) and Co3 (purple trace), measured in the presence of TEOA (0.1 M, buffered at pH 7) as hole scavenger.

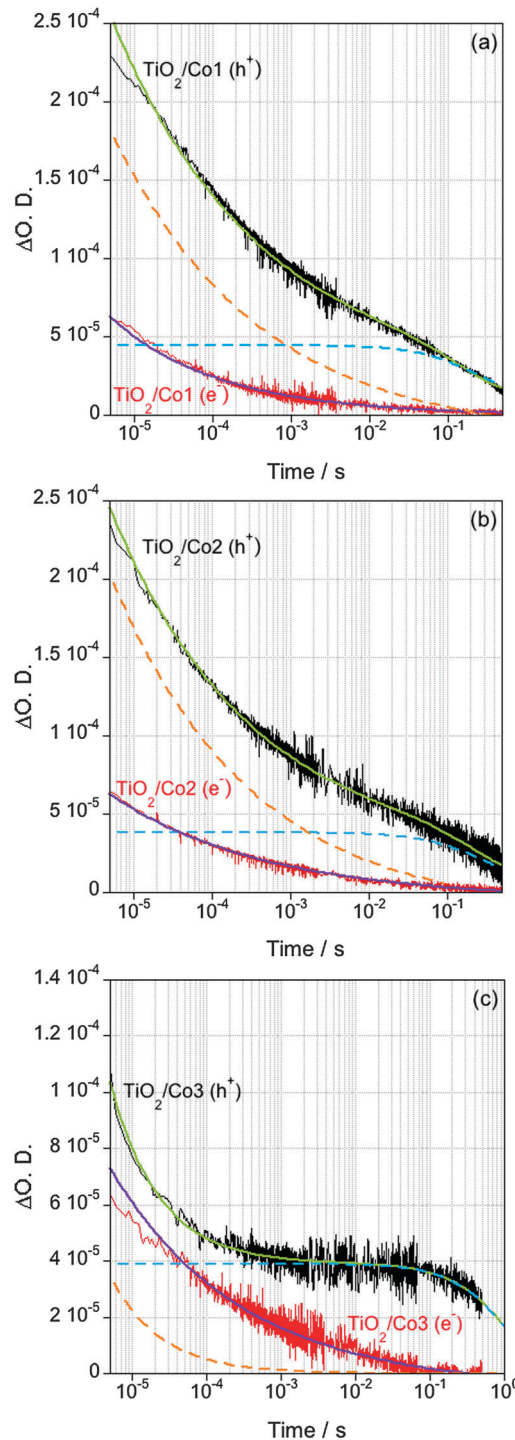


Fig. 3 TA decays of TiO<sub>2</sub> loaded with (a) Co1, (b) Co2 and (c) Co3, measured in the absence of hole scavenger. The red traces correspond to electrons, while the black traces are assigned to holes. The orange and blue dashed lines represent the power law and exponential components of the biphasic holes decay, respectively.

of electrons from the semiconductor to the molecular catalyst, whereas the holes remain in the valence band of the semiconductor. The decays of photoexcited holes are biphasic, with a fast phase ( $10^{-6}$ – $10^{-4}$  s) fitting to a power law equation and a



slow component ( $10^{-4}$ – $1$  s) fitting to a mono-exponential decay. This biphasic behaviour is clearest for **Co3**, where these two decay phases exhibit the largest difference in timescales, but is also resolved in fits to the decays for **Co1** and **Co2**, as shown by the dashed lines in Fig. 3. The fast, power law, hole decay phase exhibits similar kinetics to the decay of the electron signal at 900 nm, suggesting this phase should be assigned primarily to electron–hole recombination in the semiconductor, in competition with electron transfer to the molecular catalyst. The slow phase is assigned to recombination of long-lived holes in the valence band of the semiconductor with electrons transferred to the catalyst. The timescale of this recombination reaction between the reduced catalyst and the holes in the semiconductor varies between catalysts, taking place in  $t_{50\%} \sim 220$  ms for **Co1**, while being slower for **Co2** ( $t_{50\%} \sim 450$  ms) and **Co3** ( $t_{50\%} \sim 800$  ms) (determined from the time constant of the slow hole decay phase, see Fig. S4, ESI† for details of data fitting).

The electron transfer between the semiconductor and the molecular catalyst is expected to occur through electron tunnelling, with a rate constant ( $k_{ET}$ ) depending exponentially upon the spatial separation between the semiconductor and the redox active orbitals of the molecular catalyst ( $r$ ) – in this case, the metal centre – ( $k_{ET} \propto e^{-\beta r}$ , where  $\beta$  corresponds to the barrier height to electron tunnelling).<sup>3a,8</sup> Fig. 4 shows the linear correlation between the  $\log(1/t_{50\%})$  and  $r$  for both charge separation from  $\text{TiO}_2$  to the catalyst (Fig. 2) and the recombination reaction between the reduced catalyst and the holes accumulated in the  $\text{TiO}_2$  valence band (slow hole decay phase, Fig. 3). Comparison of the  $> 4$  fold retardation of the electron transfer kinetics yields a value for the electron tunnelling exponent ( $\beta$ ) of  $1.12 \text{ \AA}^{-1}$  for the direct electron transfer and  $0.65 \text{ \AA}^{-1}$  for the recombination reaction, lying within the calculated range for heterogeneous electron transfers through electron tunnelling across covalent

bonds ( $\sim 0.5$  to  $\sim 1 \text{ \AA}^{-1}$ ).<sup>8a,c</sup> Qualitatively similar behaviour was obtained using different kinetic analyses, with  $\beta$  ranging from  $0.91$ – $1.12 \text{ \AA}^{-1}$  for direct electron transfer and  $0.51$ – $0.65 \text{ \AA}^{-1}$  for the recombination reaction (Fig. S5 and Tables S1 and S2, ESI†). For the direct electron transfer, the value of  $\beta$  is similar to the distance dependencies observed previously for dye sensitised charge separation and recombination.<sup>8b</sup> The origin of the somewhat smaller value of  $\beta$  for the recombination electron transfer reaction is unclear, but may be related to the energetics of the bridge group and/or some structural reorientation of the catalyst following electron transfer.<sup>9</sup>

It is apparent that the kinetics of photoinduced charge separation from the  $\text{TiO}_2$  conduction band to the catalytic centre is approximately 4 orders of magnitude faster than the reverse charge recombination with valence band holes. This rectifying behaviour is clearly beneficial for device function and is analogous to the rectifying behaviour observed at dye-sensitized interfaces.<sup>8a,c</sup> The physical origin of this beneficial behaviour is not fully established. It may in part be associated with the recombination reaction lying in the Marcus inverted region (we estimate energetic driving energies for the forward and reverse electron transfer reactions of  $\sim 0.6$  and  $2.7$  eV respectively, in comparison the reorganisation energy for analogous systems is typically estimated as  $\sim 1$  eV<sup>10</sup>). It may also be associated with the relatively low density, and low mobilities, of valence band  $\text{TiO}_2$  holes. In either case, the relatively slow recombination dynamics is promising for future device development.

We note that the trends in electron transfer rate constants do not appear to correlate with differences in catalyst reduction potential. **Co3** exhibits a modestly more positive  $\text{Co}^{\text{III/II}}$  reduction potential than **Co1** and **Co2** (Table S3, ESI†). Assuming a reorganization energy of  $1$  eV,<sup>10</sup> charge separation and recombination should exhibit normal and inverted dependencies, respectively, in contrast to our observation that **Co3** exhibits slower kinetics for both reactions. Rather for the catalyst series studied herein (where the differences in reduction potential are relatively small), the primary determinant of the rate constants appears to be the tunnelling distance. A detailed analysis of this point is beyond the scope of this paper.

The results herein demonstrate that semiconductor/catalyst interfaces can be effective at achieving charge separation in hybrid systems by physically separating the charge carriers, with the holes resting in the semiconductor and the electrons being transferred away from its surface. We note that molecular catalysts are not rigid structures and a distribution of lengths might coexist, thus, the calculated distances are considered a representation of the average distribution in our systems. The increase in lifetime is achieved in the absence of band bending within the semiconductor (not present herein as the  $\text{TiO}_2$  particle diameters are less than the space charge layer depth). The carrier lifetimes are increased as the spatial distance of the catalytic site from the semiconductor surface is increased. However, for the simple catalyst series studied herein, this increased lifetime comes at the expense of slower charge separation kinetics which, in the absence of hole scavengers, reduces the yield of charge separation. Strategies to mitigate this loss of yield could include appropriate design of linker energetics, or increased driving force for charge separation. Nevertheless, the

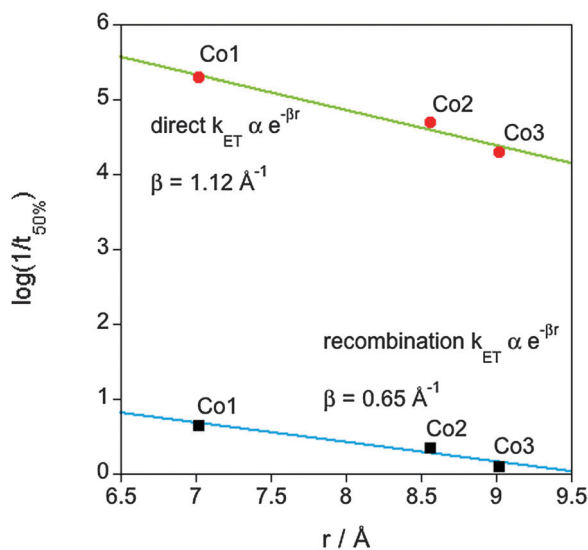


Fig. 4 Plot of the logarithm of  $1/t_{50\%}$  of the electron transfer from  $\text{TiO}_2$  to the molecular catalyst (green trace) and the recombination between the reduced catalyst and the holes accumulated in the  $\text{TiO}_2$  (blue trace) as a function of catalyst core-anchoring groups distance.



reduction in electron–hole recombination achieved with **Co3** shows a remarkable potential for its use in hybrid systems for light-driven fuel synthesis reactions.

In summary, we have demonstrated the importance of catalyst molecular design to achieve long-lived charge separated states in hybrid molecular–semiconductor systems. The key parameter controlling the kinetics of charge separation and recombination is shown to be the physical separation between the semiconductor and the catalytic core. Thus, the introduction of linkers enhancing the distance between the semiconductor and the catalytic core allows for reduced electron–hole recombination by a factor of 4. This long-lived charge separation is likely to be crucial in performing the slow multi-electron catalytic reduction reaction of protons.

Financial support from the ERC (project Intersolar to J. D.) and the EPSRC (EP/H00338X/2 to E. R.) is gratefully acknowledged. A. R. thanks the European Commission Marie Curie CIG (PhotoCO2) and E. R. the Christian Doppler Research Association (Austrian Federal Ministry of Science, Research and Economy and National Foundation for Research, Technology and Development), and the OMV Group. We thank Shababa Selim and Ernest Pastor for experimental support.

## Notes and references

‡ DFT calculations at B3LYP/6-311G(d) level of theory were performed to determine the spatial separation between the Co metal centre and phosphate groups anchoring these catalysts to the semiconductor at their most stable configuration/conformation (minimum energy).

§ The relatively large amplitude of the fast hole decay phase for **Co1** and **Co2** suggests that this decay phase may also result in part from holes recombining with a sub-population of reduced catalysts unfavourably aligned relative to the TiO<sub>2</sub> surface. The smaller amplitude of this phase for **Co3** is consistent with this catalyst employing two phosphonate linker units, ensuring alignment of all catalyst molecules normal to this surface.

- (a) P. D. Tran, L. H. Wong, J. Barber and J. S. C. Loo, *Energy Environ. Sci.*, 2012, **5**, 5902; (b) J. Yang, D. Wang, H. Han and C. Li, *Acc. Chem. Res.*, 2013, **46**, 1900; (c) J. Huang, K. L. Mulfort, P. Du and L. X. Chen, *J. Am. Chem. Soc.*, 2012, **134**, 16472; (d) A. Krawicz, J. Yang,

- Anzenberg, J. Yano, I. D. Sharp and G. F. Moore, *J. Am. Chem. Soc.*, 2013, **135**, 11861; (e) J. M. Gardner, M. Beyler, M. Karnahl, S. Tschierlei, S. Ott and L. Hammarström, *J. Am. Chem. Soc.*, 2012, **134**, 19322; (f) L. Li, L. Duan, F. Wen, C. Li, M. Wang, A. Hagfeldt and L. Sun, *Chem. Commun.*, 2012, **48**, 988; (g) M. A. Gross, A. Reynal, J. R. Durrant and E. Reisner, *J. Am. Chem. Soc.*, 2014, **136**, 356; (h) Z. Han, F. Qiu, R. Eisenberg, P. L. Holland and T. D. Krauss, *Science*, 2012, **338**, 1321; (i) C. Gimbert-Surinach, J. Albero, T. Stoll, J. Fortage, M. N. Collomb, A. Deronzier, E. Palomares and A. Llobet, *J. Am. Chem. Soc.*, 2014, **136**, 7655.
- A. Reynal, F. Lakadamyali, M. A. Gross, E. Reisner and J. R. Durrant, *Energy Environ. Sci.*, 2013, **6**, 3291.
- (a) J. N. Clifford, E. Palomares, M. K. Nazeeruddin, M. Grätzel, J. Nelson, X. Li, N. J. Long and J. R. Durrant, *J. Am. Chem. Soc.*, 2004, **126**, 5225; (b) A. Reynal, A. Fornelli, E. Martinez-Ferrero, A. Sanchez-Diaz, A. Vidal-Ferran, B. C. O'Regan and E. Palomares, *J. Am. Chem. Soc.*, 2008, **130**, 13558; (c) A. Mishra, M. K. R. Fischer and P. Bäuerle, *Angew. Chem., Int. Ed.*, 2009, **48**, 2474; (d) S. Sinn, B. Schulze, C. Friebe, D. G. Brown, M. Jäger, J. Kübel, B. Dietzek, C. P. Berlinguette and U. S. Schubert, *Inorg. Chem.*, 2014, **53**, 1637; (e) S. M. Feldt, P. W. Lohse, F. Kessler, M. K. Nazeeruddin, M. Grätzel, G. Boschloo and A. Hagfeldt, *Phys. Chem. Chem. Phys.*, 2013, **15**, 7087.
- Y. Gao, L. Zhang, X. Ding and L. Sun, *Phys. Chem. Chem. Phys.*, 2014, **16**, 12008.
- (a) F. Lakadamyali and E. Reisner, *Chem. Commun.*, 2011, **47**, 1695; (b) N. M. Muresan, J. Willkomm, D. Mersch, Y. Vaynzof and E. Reisner, *Angew. Chem., Int. Ed.*, 2012, **51**, 12749; (c) J. Willkomm, N. M. Muresan and E. Reisner, in preparation; (d) F. Lakadamyali, A. Reynal, M. Kato, J. R. Durrant and E. Reisner, *Chem. – Eur. J.*, 2012, **18**, 15464; (e) S. Ito, T. N. Murakami, P. Comte, P. Liska, C. Grätzel, M. K. Nazeeruddin and M. Grätzel, *Thin Solid Films*, 2008, **516**, 4613.
- (a) J. Tang, J. R. Durrant and D. R. Klug, *J. Am. Chem. Soc.*, 2008, **130**, 13885; (b) A. Yamakata, T.-a. Ishibashi and H. Onishi, *J. Phys. Chem. B*, 2001, **105**, 7258.
- (a) J. Nelson, *Phys. Rev. B: Condens. Matter Mater. Phys.*, 1999, **59**, 15374; (b) A. J. Cowan, J. Tang, W. Leng, J. R. Durrant and D. R. Klug, *J. Phys. Chem. C*, 2010, **114**, 4208.
- (a) J. F. Smalley, S. W. Feldberg, C. E. D. Chidsey, M. R. Linford, M. D. Newton and Y.-P. Liu, *J. Phys. Chem.*, 1995, **99**, 13141; (b) S. A. Haque, S. Handa, K. Peter, E. Palomares, M. Thelakkat and J. R. Durrant, *Angew. Chem., Int. Ed.*, 2005, **44**, 5740; (c) R. J. D. Miller, G. L. McLendon, A. J. Nozik, W. Schmickler and F. Willig, *Surface electron transfer processes*, VCH, New York, 1995.
- J. R. Winkler and H. B. Gray, *J. Am. Chem. Soc.*, 2014, **136**, 2930.
- B. H. Solis and S. Hammes-Schiffer, *Inorg. Chem.*, 2011, **50**, 11252.

